Circularly polarized luminescence of encaged Eu(iii) and Tb(iii) complexes controlled by an inherently chiral remote unit

Estelle Godart, Oriane Della-Negra, Augustin Long, Alberto Insuasty, Lorenzo Arrico, Costanza Benetti, Elise Antonetti, Paola Nava, Yoann Cotelle, Nicolas Vanthuyne, et al.

Circularly polarized luminescence of encaged Eu(III) and Tb(III) complexes controlled by an inherently chiral remote unit†

Estelle Godart,‡[a] Oriane Della-Negra,‡[a] Augustin Long,[a] Alberto Insuasty,[a] Lorenzo Arrico,[b] Costanza Benetti,[b] Elise Antonetti,[a] Paola Nava,[a] Yoann Cotelle,[a] Nicolas Vanthuyne,[a] Marion Jean,[a] Simon Pascal,[c] Jean-Pierre Dutasta,*[d] Lorenzo Di Bari*[b] and Alexandre Martinez*[a]

A molecular cage-based approach to obtain enantiopure lanthanide complexes with circular polarized luminescence (CPL) activities is presented. Hemicryptophane endohedral complexes were designed by functionalizing the molecular cage with pyridine-2,6-dipicolinamide coordinating groups. Taking advantage of the ability of the inherent chirality of the remote cyclotriveratrylene (CTV) unit to propagate along the linkers of the molecular cage, the encapsulated lanthanide complexes with a controlled chirality have been obtained. In this way, we obtained the CPL active Tb(III) and Eu(III) cages although the chiral CTV unit is located far from the complexation sites. This opens the way for a broader use of enantiopure covalent cages for CPL applications.

Circular polarized luminescence (CPL) refers to the differential emission of right and left circularly polarized light by chiral non-racemic luminescent systems.[1] CPL is defined as the difference between the intensities of the left (I_L) and right (I_R) circularly polarized emitted light (I_L) (CPL = $\Delta I = I_L - I_R$). The luminescence dissymmetry factor g_{lum} (eqn (1)) is used to quantify to what extent the intensity of the right or left circular polarized light is emitted preferentially over the other.

$$g_{lum} = \frac{2(I_L - I_R)}{(I_L + I_R)} \quad (1)$$

Typically, organic molecules display g_{lum} values in the range of 10^{-3}–10^{-2}, whereas lanthanide complexes can exhibit g_{lum} factors up to 0.1–1, with the exceptional value of about |1.4| for $CsEu(hfbc)_4$ being the highest g_{lum} reported to date.[2] In addition, luminescent lanthanide complexes present intriguing photophysical properties, such as narrow emission bands at almost fixed wavelength and long lifetimes (up to ms). The combination of all these aspects makes chiral emissive lanthanide complexes particularly suitable as CPL emitters for a plethora of applications. In fact, lanthanide-based CPL arouses a considerable interest in different scientific and technological fields, such as in the development of (chiro)optical probes of chiral molecules and biological systems,[3] information storage techniques,[4] and circularly polarized light-emitting diodes (CP-OLEDs).[5]

Various chiral structures like podands or macrocycles,[6] including pillar[*n*]arenes[7] or cyclophanes,[8] helicenes,[9] binaphthyl derivatives,[10] cubes,[11] porphyrin nanorings[12] or rotaxanes,[13] have been reported to show CPL properties. Recently, some of us reported the first investigation of the CPL activity of Eu^{3+} and Sm^{3+} cryptates, demonstrating that the encapsulation of the lanthanide ions in the cavity of a rigid chiral tris-bipyridyl based cryptand is indeed an efficient tool to obtain stable Ln^{3+} complexes endowed with circularly polarized emission.[14] In this direction, the design of new chiral molecular cage architectures and the investigation of other lanthanide ions appear to be fundamental for the development of such promising class of lanthanide complexes.[15]

The preorganisation and rigidity of the cage ligand should efficiently control the configuration at the lanthanide center, thus translating into interesting CPL properties. In this specific case, *i.e.* with lanthanide ions, the synthesis of endohedrally

[a] *Aix Marseille Univ., CNRS, Centrale Marseille, iSm2, UMR 7313, 13397, Marseille, France. E-mail: alexandre.martinez@centrale-marseille.fr*
[b] *Dipartimento di Chimica e Chimica Industriale, Università di Pisa, Via Moruzzi 13, 56124 Pisa, Italy. E-mail: lorenzo.dibari@unipi.it*
[c] *Aix Marseille Univ, CNRS UMR 7325, CINaM, Campus de Luminy, case 913, 13288 Marseille cedex 09, France*
[d] *ENSL, CNRS, Laboratoire de Chimie UMR 5182, 46 allée d'Italie, F-69364 Lyon, France*

† Electronic supplementary information (ESI) available. See DOI: https://doi.org/10.1039/d2nj02360a

‡ Co-first authors.

functionalized enantiopure chiral molecular cages is a challenging task, given the high number of Lewis base sites required to fully saturate the coordination sphere of the Ln^{3+} ions. The introduction of stereogenic units in the vicinity of the coordination sites of the molecular cage is expected to favor the chiral transfer, but it appears hard to be achieved with bowl-shaped cage ligands. In this context, another strategy could be the use of a remote stereogenic unit included in the architecture of the molecular cage, which is able to induce a well-defined chiral conformation to the rest of the molecule. Among this kind of chiral molecular cages, hemicryptophanes are promising candidates.[16] Such systems combine a chiral CTV moiety facing another C_3 symmetrical unit. They can be easily endohedrally functionalized, synthesized enantiomerically pure on gram scale, and the CTV unit is able to efficiently control the chiral arrangement of the arms and of the other linked C_3 symmetry unit.[17] This prompted us to examine the ability of enantiomerically pure Ln(III)@hemicryptophane complexes to display CPL properties. Herein, we report the synthesis of the enantiopure hemicryptophane cage **12** presenting nine coordination sites oriented inward its cavity (Scheme 1). The (±)-**12** racemic mixture was resolved by chiral HPLC and the assignment of the absolute configuration of the enantiomeric ligands was achieved from their ECD spectra. The related Eu^{3+} and Tb^{3+} complexes display substantial g_{lum} values.

Results and discussion

Compound **5** was synthesized in four steps, starting from vanillyl alcohol **1** (Scheme 1).[18] The phenol unit was first alkylated with dibromoethane, and then the alcohol function was protected using a THP group, providing compound **3** in 43% yield (two steps). Compound **3** reacted with sodium azide in DMF to give **4** in almost quantitative yield. A subsequent Staudinger reaction afforded the expected key intermediate **5** in 76% yield. We then chose to de-symmetrize the commercially available pyridine-2,6-dicarboxylic acid **6** following the

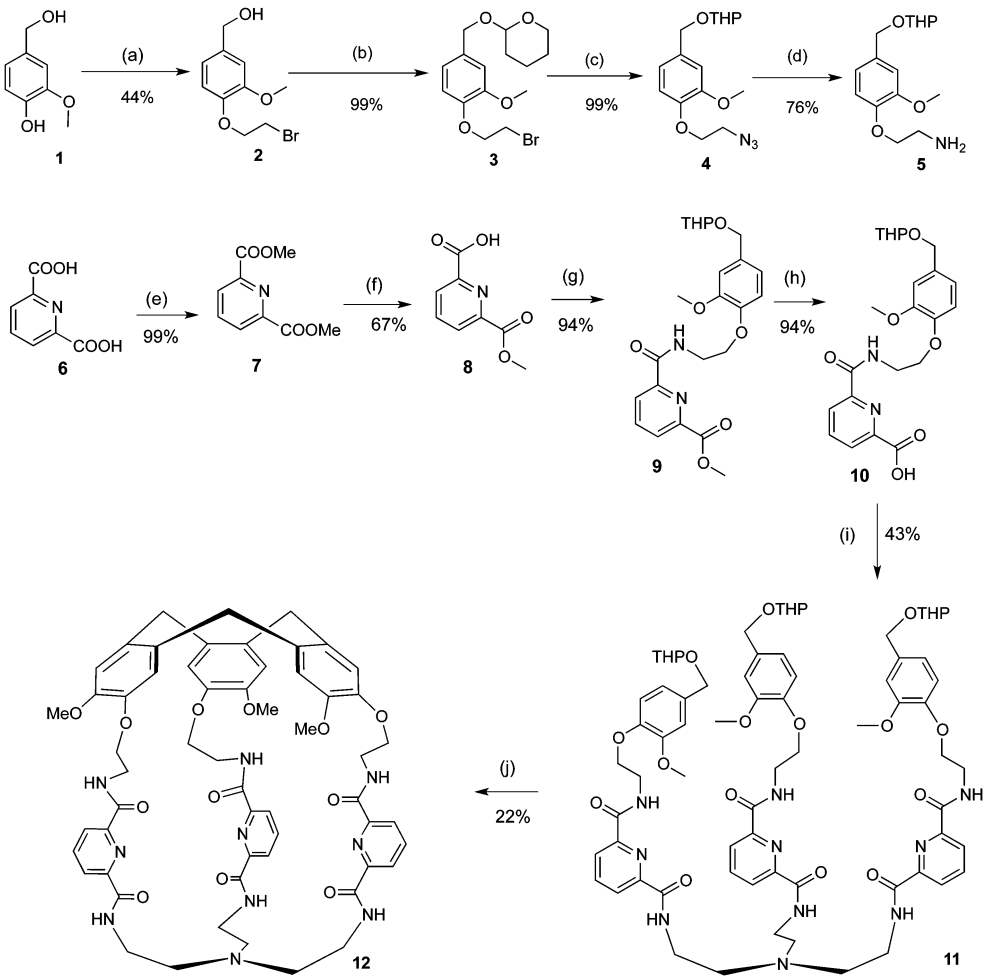

Scheme 1 Synthesis of hemicryptophane **12**. *Reaction conditions*: (a) dibromoethane, K_2CO_3, EtOH, reflux, 6 h; (b) DHP, PPTS, THF/DCM (1/1), rt, 18 h; (c) NaN_3, DMF, 60 °C, 5 h; (d) PPh_3, THF/H_2O (30/1) 0 °C to rt, 24 h; (e) MeOH, reflux, H_2SO_4, 12 h; (f) KOH (1 equiv.), MeOH, 0 °C, 2 h, then rt, 12 h; (g) **5** (1 equiv.), PyBOP (1 equiv.), NMM (1.5 equiv.), DMF, rt, 12 h; (h) LiOH (2.5 equiv.), MeOH, rt, 12 h; (i) tren (0.3 equiv.), HOBt (3 equiv.), DCC (3 equiv.) DIPEA (10 equiv.), CH_3CN, rt, 12 h); (j) HCOOH, $CHCl_3$, rt, 24 h.

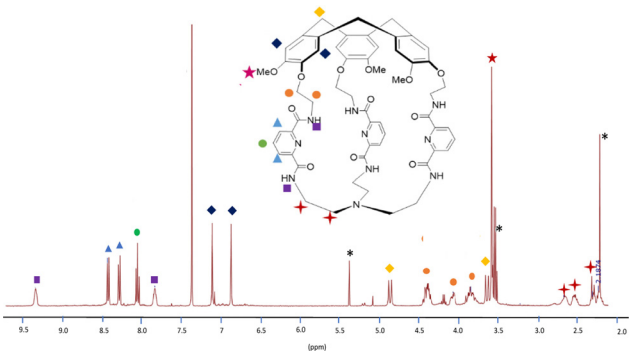

Fig. 1 ^{1}H NMR spectrum (400 MHz, 298K, $CDCl_3$) of cage **12** (* = solvent).

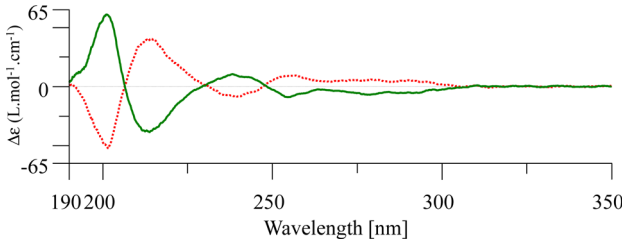

Fig. 2 Experimental ECD spectra of the enantiomers of **12**: the first eluted enantiomer ((+)-**12**) is represented with a green solid line (0.092 mM in CH_3CN); and the second one ((−)-**12**), by a red dotted line (0.092 mM in CH_3CN).

procedure described by Shmuck *et al.*: esterification of the starting material **6** in methanol, using H_2SO_4 as catalyst, gave the di-ester **7**, which was selectively mono-saponified allowing us to isolate **8** with 66% yield (over the two steps).[19] The coupling of intermediate **5** and **8** was then performed in DMF using ByBOP as coupling agent. The resulting compound **9** was thus obtained in 94% yield, and its ester function was saponified to provide **10** in 94% yield. This compound then reacted with the tris(2-aminoethyl)amine (tren) unit, using DCC and HOBt as coupling agents and DIPEA as base to afford the precursor **11**. The last macrocyclization step was achieved by diluting (10^{-3} M) the precursor **11** in a formic acid/chloroform 1 : 1 mixture. Thus, hemicryptophane **12** was obtained with an overall yield of 5.5%, following the 10-steps synthetic pathway. The ^{1}H NMR spectrum of **12** is shown in Fig. 1. Well-defined, sharp and identical signals are observed for the protons of the three arms, evidencing that the cage displays in solution an average structure with C_3 symmetry. The spectrum shows the expected signals for the CTV moiety: two doublets at 3.59 and 4.77 ppm for the diastereotopic protons of the $ArCH_2$ bridges, one singlet at 3.52 ppm corresponding to the OMe protons and two singlets at 7.01 and 6.77 ppm for the aromatic protons. The signals of the protons of the three pyridine rings appear as two doublets and one triplet at 8.32, 8.16 and 7.94 respectively. The diastereotopic protons of the $-OCH_2CH_2N-$ and $-NCH_2CH_2N-$groups included in the arms give two sets of rather complex pattern between 4.4–3.6 ppm and 2.7–2.1 ppm, respectively. The signals of the two NH amides appear as broad peaks at 9.22 and 7.73 ppm.

Resolution of the racemic mixture of cage **12** was performed by chiral HPLC using a chiralpak IE column and EtOH/$CHCl_3$ (7 : 3) as eluent (Fig. S13, ESI†). This afforded the (−)- and (+)-enantiomers with ee > 99.5% and 98.5%, respectively (Fig. S14 and S15, ESI†). The assignment of the absolute configuration of each enantiomer was carried out through the comparison of their ECD spectra recorded in CH_2Cl_2 at 298 K (Fig. 2) with those of previously reported hemicryptophanes and CTVs.[20] Indeed, Collet *et al.* demonstrated that the $^{1}L_a$ transition area (240 nm) is poorly sensitive to the nature of the substituent;[21] thus, a direct comparison of the ECD spectra allowed us to determine the absolute configuration of our CTV-based compounds. In agreement with these previous works, the first eluted compound (+)-**12** has the *P* configuration, whereas the second eluted (−)-**12** has the *M* configuration.

The La(III)@**12**, Eu(III)@**12** and Tb(III)@**12** complexes were then synthesized by mixing 1 equiv. of cage ligand with 1 equiv. of the corresponding metal triflate salt in methanol in the presence of an excess of NEt_3 at 60 °C for 24 h. The ^{1}H NMR spectra of the ligand (Fig. 1) and of the complexes (Fig. 3) exhibit single sets of resonances, which confirm an average C_3 symmetry in solution for the free ligand and its Ln complexes.

Furthermore, upon complexation, only one diastereomer is formed, highlighting the ability of the chirality of the CTV unit to propagate around its linkers and to control the *Δ* or *Λ* configuration of the chiral metal center, as previously observed for other hemicryptophane derivatives. Density Functional Theory calculations were performed to get some insights on the possible structures of a Ln(III)@**12** complex, containing the

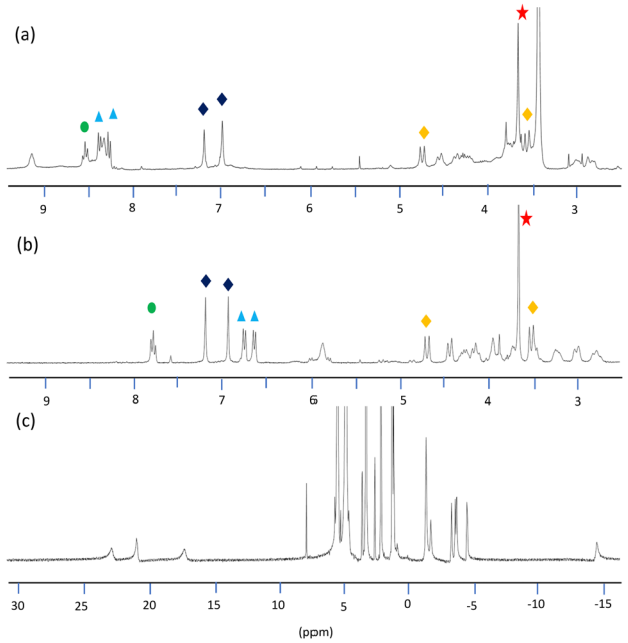

Fig. 3 ^{1}H NMR (400 MHz, 298 K, CD_3CN) of (a) La(III)@**12**; (b) Eu(III)@**12** and (c) Tb(III)@**12**. Some characteristic signals are highlighted for the La(III)@**12** and Eu(III)@**12** complexes: (i) for the CTV unit (CH_2 bridges ◆, OMe ★, aromatic protons ◆) and (ii) for the pyridine moieties (protons in meta ▲ and para position ●).

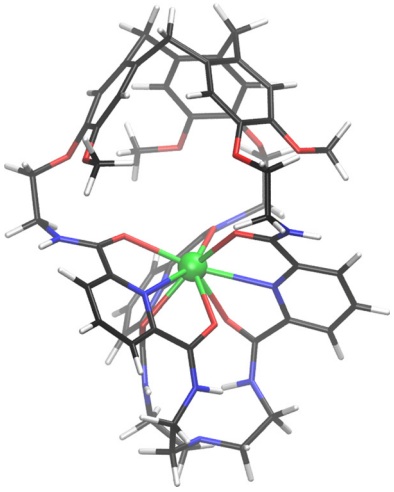

Fig. 4 Computed structure (BP86-D3/def2-SVP) of the diastereomer *P*–*Λ* of the complex La(III)@**12**.

analogous La^{3+} cation. The most stable structure we have calculated keeping C_3 symmetry corresponds to the *P*–*Λ* diastereomer, the *M*–*Λ* diastereomer being 43 kJ mol^{-1} higher in energy (Fig. 4 and Fig. S22, S23, ESI†). This is in agreement with the presence of a single species and with a single set of signals observed in the ^{1}H NMR spectrum. The cation is stabilized by interactions with the lone pairs of the heteroatoms available on the linkers of the cage connecting the CTV and tren units. The La^{3+} ion is coordinated by the nitrogen atoms of the three pyridines (La···N distances = 281 pm) and by the oxygen atoms of the carbonyl groups (La···O distances = 251 and 258 pm), achieving the usual 9-fold coordination pattern. The energy decomposition analysis reveals that the largest contribution to the interaction energy between the cage and the metal is indeed due to the electrostatic term. The large magnetic susceptibility anisotropy of Tb^{3+} induces a very significant shift of the ^{1}H-NMR signals, which span about 40 ppm. At the same time, the lines appear well-recognizable and relatively narrow, demonstrating that there is no exchange broadening. This confirms that the hemicryptophane rigidly encages the lanthanide and shelters it from the environment.[22]

Ethanol solution of Tb(III)@**12** and Eu(III)@**12** exhibit the typical red and green emissions upon UV irradiation (365 nm). The emission spectra of the complexes in solution are shown in Fig. 5. In the case of Tb(III)@**12** the bands are associated to the $^5D_4 \rightarrow {}^7F_6$ and $^5D_4 \rightarrow {}^7F_5$ transitions centred at *ca.* 490 nm and *ca.* 545 nm, respectively, whereas in the case of Eu@**12** the narrow bands are related to the $^5D_0 \rightarrow {}^7F_1$ (*ca.* 595 nm) and to the $^5D_0 \rightarrow {}^7F_2$ (*ca.* 615 nm). In all cases the total emission spectra do not show any fine structure and should be considered as the envelope of more complex term-to-term multiplets. The luminescence quantum yields of Eu(III)@**12** and Tb(III)@**12** were measured in ethanol solutions, revealing weak values of *ca.* 0.5% and 2.6%, respectively. These quantum yields are higher than the absolute yields obtained for the Eu(III) and Tb(III) complexes parents lacking cavity.[23] The cage structure could prevent external interactions and the related deactivation pathway that are more likely to occur with their podand analogues. The emission decay was also evaluated, showing luminescence lifetimes of 0.39 ms and 0.97 ms for Eu(III)@**12** and Tb(III)@**12**, respectively (see Fig. S18, ESI†). These data also support the formation of a single species in each case, in agreement with the mass spectra (Fig. S12 and S14, ESI†).

The CPL spectra of Tb(III)@**12** and Eu(III)@**12** are reported in Fig. 6. The spectra were recorded in ethanol by irradiating the samples at 365 nm. Tb(III)@(+)-**12**, Tb(III)@(−)-**12** and Eu(III)-(−)-**12** complexes gave rise to non-zero CPL signals, confirming in all cases the presence of a chiral lanthanide emitting species.

More in details, the CPL spectra of the two enantiomers of Tb(III)@**12** are specular, as expected for a couple of enantiomers. The highest g_{lum} factor for each enantiomer was recorded for the most-blue shifted component of the $^5D_4 \rightarrow {}^7F_5$ multiplet (centered at 545 nm) and amounts to +0.11 for Tb(III)@(+)-**12** and −0.13 for Tb(III)@(−)-**12**. Interestingly, the oppositely signed bands of CPL spectra reveal partial resolution of the M_J-components (neglecting hot bands, $^5D_4 \rightarrow {}^7F_6$ and $^5D_4 \rightarrow {}^7F_5$ should originate 6- and 5-fold multiplets, respectively).

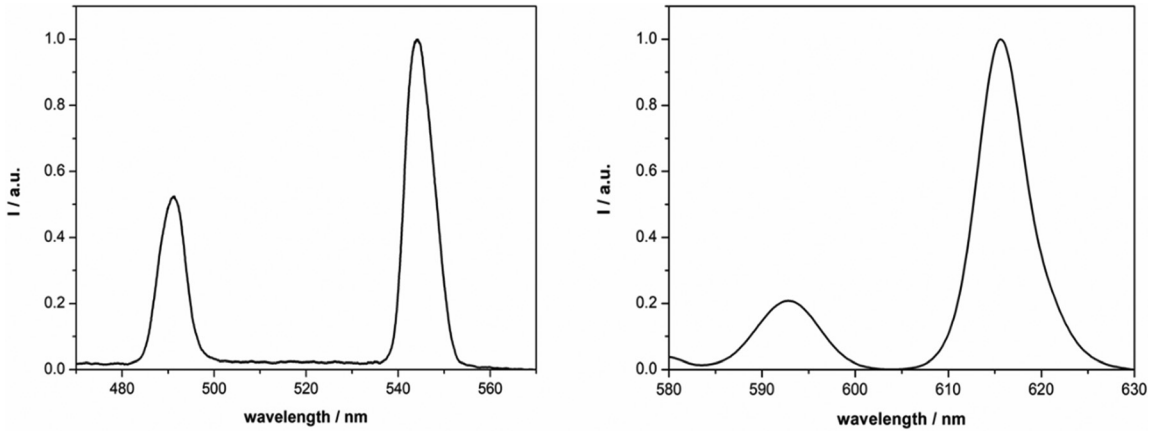

Fig. 5 Emission spectra of Tb(III)@**12** (left) and Eu(III)@**12** (right). The spectra were normalized to the most intense band (λ_{exc} = 365 nm).

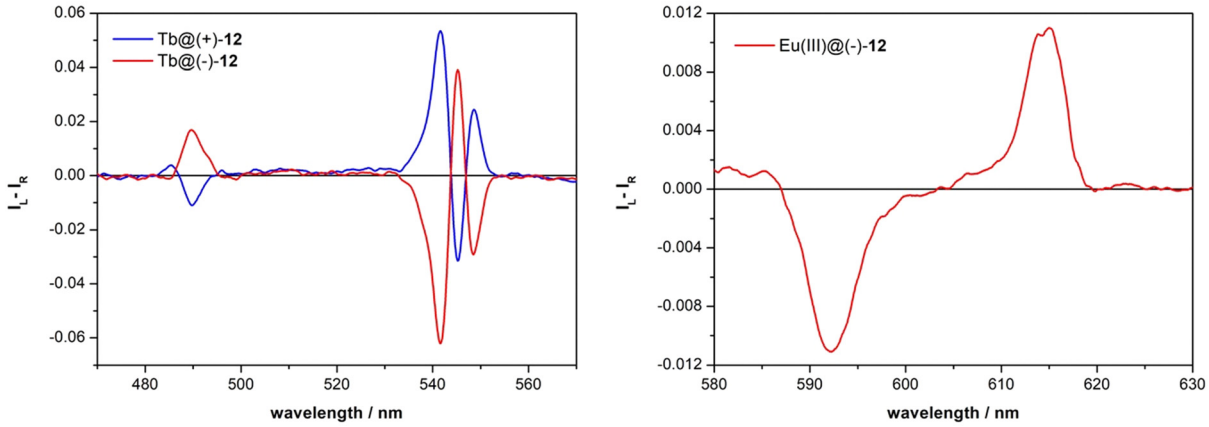

Fig. 6 Left: CPL spectra of Tb(III)@(+)-12 (blue line) and Tb(III)@(−)-**12** (red line). Right: CPL spectrum of Eu(III)@(−)-**12** in EtOH at 298 K. The CPL spectra are normalized to the most intense band of the relative emission spectrum.

In the case of Eu(III), only one enantiomer was synthesized, namely the Eu(III)@(−)-**12** complex. It shows two oppositely signed CPL bands in the region 580–630 nm, corresponding to $^5D_0 \rightarrow {}^7F_1$ (*ca.* 595 nm) and to $^5D_0 \rightarrow {}^7F_2$ (*ca.* 615 nm) transitions. The highest g_{lum} factor (−0.05) was observed for the former. Interestingly, these two bands show approximately equal and opposite rotational strengths, which indicates a larger contribution of the dynamic coupling rather than static coupling mechanism as the origin of the CPL signal. The static coupling is mainly related to the chirality of the first coordination sphere of Ln(III) and it is expected to be vanishingly small for achiral coordination polyhedra. Presently, this would indicate that the six oxygen atoms of the amide groups would be arranged close to a trigonal antiprism. The dynamic coupling arises because the electric dipole transition moments of the dipicolinamide chromophores couple with the magnetic dipole transition moments allied with Eu(III) f–f transitions. The skew angle between C2 and C6 of a dipicolinamide and the C_3 main symmetry axis in trigonal antiprismatic coordination would fully justify an efficient dynamic coupling. Unlike Tb(III)@(−)-**12**, the Eu(III)@(−)-**12** complex displays no fine structure in its CPL spectrum.

Conclusions

In conclusion, we have reported the 10-steps synthesis of the enantiomerically pure covalent cage **12** that presents nine coordination sites for lanthanide ions complexation. The absolute configuration of the ligand **12** was assigned by ECD spectroscopy. According to their NMR spectra, the corresponding lanthanide complexes were obtained as a single diastereomer, suggesting that the remote chirality of the CTV unit propagate along the linkers to control the chirality at the metal center. In this way, we obtained the first example of a CPL active encapsulated Tb(III) complex. While the corresponding Eu(III) complex showed a low value of g_{lum} value, the Tb(III)@**12** compound revealed itself to be endowed with a high value of g_{lum} (up to $|0.13|$). In the context of CPL emitters, this finding can open new ways for the design of new enantiopure molecular cages suitable for CPL applications.

1 (*a*) J. P. Riehl and G. Muller, in *Comprehensive Chiroptical Spectroscopy: Instrumentation, Methodologies, and Theoretical Simulations*, ed. N. Berova, P. L. Polavarapu, K. Nakanishi and R. W. Woody, John Wiley & Sons, 2012, vol. 1, pp. 65–90; (*b*) J. P. Riehl and F. S. Richardson, *Chem. Rev.*, 1986, **86**, 1–16.

2 (*a*) J. L. Lunkley, D. Shirotani, K. Yamanari, S. Kaizaki and G. Muller, *Inorg. Chem.*, 2011, **50**, 12724–12732; (*b*) J. L. Lunkley, D. Shirotani, K. Yamanari, S. Kaizaki and G. Muller, *J. Am. Chem. Soc.*, 2008, **130**, 13814–13815.

3 (*a*) R. Carr, N. H. Evans and D. Parker, *Chem. Soc. Rev.*, 2012, **41**, 7673–7686; (*b*) J. Yuasa, T. Ohno, H. Tsumatori, R. Shiba, H. Kamikubo, M. Kataoka, Y. Hasegawa and T. Kawai, *Chem. Commun.*, 2013, **49**, 4604–4606; (*c*) M. Leonzio,

A. Melchior, G. Faura, M. Tolazzi, M. Bettinelli, F. Zinna, L. Arrico, L. Di Bari and F. Piccinelli, *New J. Chem.*, 2018, **42**, 7931–7939; (*d*) G. Muller, *Dalton Trans.*, 2009, 9692–9707.

4 (*a*) J. Yuasa, T. Nakagawa, Y. Kita, A. Kaito and T. Kawai, *Chem. Commun.*, 2017, **53**, 6748–6751; (*b*) A. T. Frawley, A. Pal and D. Parker, *Chem. Commun.*, 2016, **52**, 13349–13352; (*c*) P. Kumar, S. Singh and B. K. Gupta, *Nanoscale*, 2016, **8**, 14297–14340.

5 (*a*) F. Zinna and L. Di Bari, *Lanthanide-Based Multifunctional Materials – From OLEDs to SIMs*, Elsevier Inc., 2018, pp. 171–194; (*b*) F. Zinna, M. Pasini, F. Galeotti, C. Botta, L. Di Bari and U. Giovanella, *Adv. Funct. Mater.*, 2017, **27**, 1603719; (*c*) F. Zinna, U. Giovanella and L. Di Bari, *Adv. Mater.*, 2015, **27**, 1791–1795.

6 (*a*) S. Tong, J.-T. Li, D.-D. Liang, Y.-E. Zhang, Q.-Y. Feng, X. Zhang, J. Zhu and M.-X. Wang, *J. Am. Chem. Soc.*, 2020, **142**, 14432–14436; (*b*) S. P. Morcillo, D. Miguel, L. Alvarez de Cienfuegos, J. Justicia, S. Abbate, E. Castiglioni, C. Bour, M. Ribagorda, D. J. Ćardenas, J. M. Paredes, L. Crovetto, D. Choquesillo-Lazarte, A. J. Mota, M. C. Carreño, G. Longhi and J. M. Cuerva, *Chem. Sci.*, 2016, **7**, 5663–5670; (*c*) P. Reine, A. G. Campaña, L. Alvarez de Cienfuegos, V. Blanco, S. Abbate, A. J. Mota, G. Longhi, D. Miguel and J. M. Cuerva, *Chem. Commun.*, 2019, **55**, 10685–10688; (*d*) K. Zhu, K. Kamochi, T. Kodama, M. Tobisu and T. Amaya, *Chem. Sci.*, 2020, **11**, 9604–9610; (*e*) A. Homberg and J. Lacour, *Chem. Sci.*, 2020, **11**, 6362–6369; (*f*) A. Homberg, E. Brun, F. Zinna, S. Pascal, M. Gorecki, L. Monnier, C. Besnard, G. Pescitelli, L. Di Bari and J. Lacour, *Chem. Sci.*, 2018, **9**, 7043–7052; (*g*) X.-N. Han, Y. Han and C.-F. Chen, *J. Am. Chem. Soc.*, 2020, **142**, 8262–8269; (*h*) J. A. Adewuyi, N. D. Schley and G. Ung, *Inorg. Chem. Front.*, 2022, **9**, 1474–1480.

7 (*a*) H. Zhu, Q. Li, B. Shi, H. Xing, Y. Sun, S. Lu, L. Shangguan, X. Li, F. Huang and P. J. Stang, *J. Am. Chem. Soc.*, 2020, **142**, 17340–17345; (*b*) J.-F. Chen, X. Yin, B. Wang, K. Zhang, G. Meng, S. Zhang, Y. Shi, N. Wang, S. Wang and P. Chen, *Angew. Chem., Int. Ed.*, 2020, **59**, 11267–11272.

8 (*a*) K. Senthilkumar, M. Kondratowicz, T. Lis, P. J. Chmielewski, J. Cybińska, J. L. Zafra, J. Casado, T. Vives, J. Crassous, L. Favereau and M. Stępień, *J. Am. Chem. Soc.*, 2019, **141**, 7421–7427; (*b*) Y. Morisaki, M. Gon, T. Sasamori, N. Tokitoh and Y. Chujo, *J. Am. Chem. Soc.*, 2014, **136**, 3350–3353; (*c*) S. K. Keshri, A. Takai, T. Ishizuka, T. Kojima and M. Takeuchi, *Angew. Chem., Int. Ed.*, 2020, **59**, 5254–5258.

9 (*a*) E. S. Gauthier, L. Abella, N. Hellou, B. Darqui, E. Caytan, T. Roisnel, N. Vanthuyne, L. Favereau, M. Srebro-Hooper, J. A. G. Williams, J. Autschbach and J. Crassous, *Angew. Chem., Int. Ed.*, 2020, **59**, 8394–8400; (*b*) K. Dhbaibi, L. Favereau, M. Srebro-Hooper, C. Quinton, N. Vanthuyne, L. Arrico, T. Roisnel, B. Jamoussi, C. Poriel, C. Cabanetos, J. Autschbach and J. Crassous, *Chem. Sci.*, 2020, **11**, 567–576; (*c*) K. Dhbaibi, L. Favereau and J. Crassous, *Chem. Rev.*, 2019, **119**, 8846–8953; (*d*) E. S. Gauthier, R. Rodriguez and J. Crassous, *Angew. Chem., Int. Ed.*, 2020, **59**, 2–19; (*e*) R. Duwald, J. Bosson, S. Pascal, S. Grass, F. Zinna, C. Besnard, L. Di Bari, D. Jacquemin and J. Lacour, *Chem. Sci.*, 2020, **11**, 1165–1169; (*f*) E. S. Gauthier, N. Hellou, E. Caytan, S. Del Fré, V. Dorcet, N. Vanthuyne, L. Favereau, M. Srebro-Hooper, J. A. G. Williams and J. Crassous, *Inorg. Chem. Front.*, 2021, **8**, 3916–3925.

10 (*a*) K. Takaishi, K. Iwachido and T. Ema, *J. Am. Chem. Soc.*, 2020, **142**, 1774–1779; (*b*) Y. Zhou, H. Li, T. Zhu, T. Gao and P. Yan, *J. Am. Chem. Soc.*, 2019, **141**, 19634–19643; (*c*) C. Maeda, K. Ogawa, K. Sadanaga, K. Takaishi and T. Ema, *Chem. Commun.*, 2019, **55**, 1064–1067.

11 H. Qu, Y. Wang, Z. Li, X. Wang, H. Fang, Z. Tian and X. Cao, *J. Am. Chem. Soc.*, 2017, **139**, 18142–18145.

12 C. Maeda, S. Toyama, N. Okada, K. Takaishi, S. Kang, D. Kim and T. Ema, *J. Am. Chem. Soc.*, 2020, **142**, 15661–15666.

13 A. H. G. David, Rl Casares, J. M. Cuerva, A. G. Campaña and V. Blanco, *J. Am. Chem. Soc.*, 2019, **141**, 18064–18074.

14 E. Kreidt, L. Arrico, F. Zinna, L. Di Bari and M. Seitz, *Chem. – Eur. J.*, 2018, **24**, 13556–13564.

15 (*a*) X.-Z. Li, C.-B. Tian and Q.-F. Sun, *Chem. Rev.*, 2022, **122**, 6374–6458; (*b*) H.-Y. Wong, W.-S. Lo, K.-H. Yim and G.-L. Law, *Chem*, 2019, **5**, 3058–3095.

16 D. Zhang, A. Martinez and J.-P. Dutasta, *Chem. Rev.*, 2017, **117**, 4900–4942.

17 (*a*) J.-P. Dutasta and A. Martinez, *ChemPlusChem*, 2020, **85**(5), 977–984; (*b*) G. Qiu, P. Nava, C. Colomban and A. Martinez, *Front. Chem.*, 2020, **8**, 994–999; (*c*) C. Colomban, B. Chatelet and A. Martinez, *Synthesis*, 2019, 2081–2099.

18 E. Godart, A. Long, R. Rosas, G. Lemercier, M. Jean, S. Leclerc, S. Bouguet-Bonnet, C. Godfrin, L.-L. Chapellet, J.-P. Dutasta and A. Martinez, *Org. Lett.*, 2019, **21**, 1999–2003.

19 C. Schmuck and U. Machon, *Chem. – Eur. J.*, 2005, **11**, 1109–1118.

20 (*a*) A. Long, O. Perraud, M. Albalat, V. Robert, J.-P. Dutasta and A. Martinez, *J. Org. Chem.*, 2018, **83**, 6301–6306; (*b*) D. Zhang, J.-C. Mulatier, J. R. Cochrane, L. Guy, G. Gao, J.-P. Dutasta and A. Martinez, *Chem. – Eur. J.*, 2016, **22**, 8038–8042.

21 J. Canceill, A. Collet, J. Gabard, G. Gottarelli and G. P. Spada, *J. Am. Chem. Soc.*, 1985, **107**, 1299–1308.

22 L. Di Bari and P. Salvadori, *Coord. Chem. Rev.*, 2005, **24**, 2854–2879.

23 F. Renaud, C. Piguet, G. Bernardinelli, J.-C. G. Bünzli and G. Hopfgartner, *J. Am. Chem. Soc.*, 1999, **121**, 9326–9342.